# Supplementary Information

## Design, synthesis, and biological evaluation of novel halogenated chlorido[*N,N′*-bis(salicylidene)-1,2-bis(3-methoxyphenyl)ethylenediamine]iron(III) complexes as anticancer agents

**Astrid Dagmar Bernkop-Schnürch[1]**, Klaus Huber[1], Armida Clauser[1,2], Monika Cziferszky[1], Daniel Leitner[3], Heribert Talasz[4], Martin Hermann[5], Stephan Hohloch[3], Ronald Gust[1], Brigitte Kircher[*2,6]

[1]Department of Pharmaceutical Chemistry, Institute of Pharmacy, CMBI—Center for Molecular Biosciences Innsbruck, CCB—Center for Chemistry and Biomedicine, University of Innsbruck, Innrain 80-82, 6020 Innsbruck, Austria

[2]Immunobiology and Stem Cell Laboratory, Department of Internal Medicine V (Hematology and Oncology), Medical University of Innsbruck, Anichstraße 35, 6020 Innsbruck, Austria

[3]Department of General, Inorganic and Theoretical Chemistry, University of Innsbruck, Innrain 80-82, 6020 Innsbruck, Austria

[4]Biocenter, Institute of Medical Biochemistry, Protein Core Facility, Medical University of Innsbruck, Innrain 80-82, 6020 Innsbruck, Austria

[5]Department of Anesthesiology and Critical Care Medicine, Medical University of Innsbruck, Anichstraße 35, 6020 Innsbruck, Austria

[6]Tyrolean Cancer Research Institute, Innrain 66, 6020 Innsbruck, Austria

*__Correspondence__

brigitte.kircher@i-med.ac.at

**Table of Content**

## 1. Characterisation of the ligands L1 – L3

1.1. $^1$H NMR spectra of the ligands

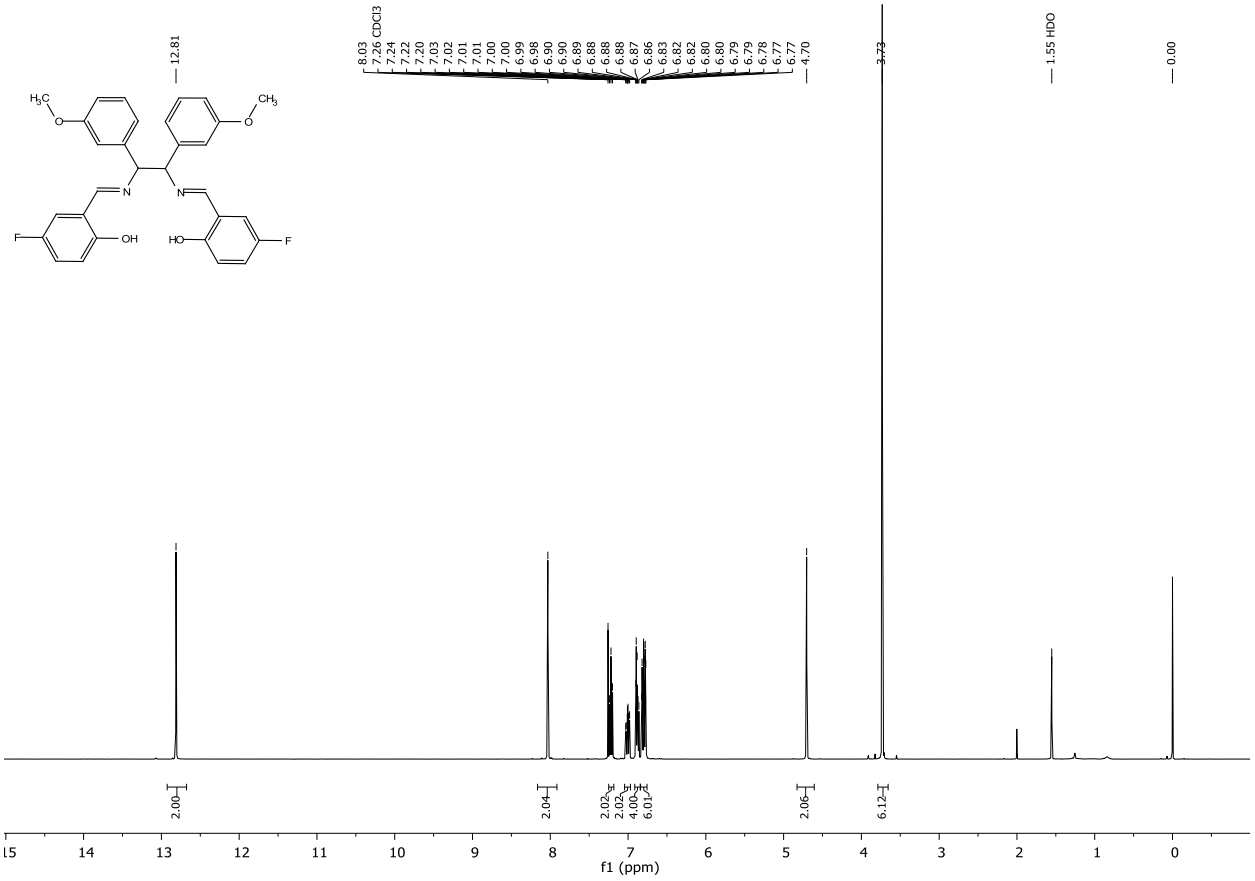


**Figure S1:** $^1$H NMR of **L1** in $CDCl_3$

$^1$H NMR (400 MHz, $CDCl_3$-*d*) δ 12.81 (s, 2H), 8.03 (s, 2H), 7.22 (t, *J* = 7.9 Hz, 2H), 7.01 (ddd, *J* = 9.1, 8.1, 3.1 Hz, 2H), 6.92 – 6.84 (m, 4H), 6.84 – 6.75 (m, 6H), 4.70 (s, 2H), 3.73 (s, 6H)

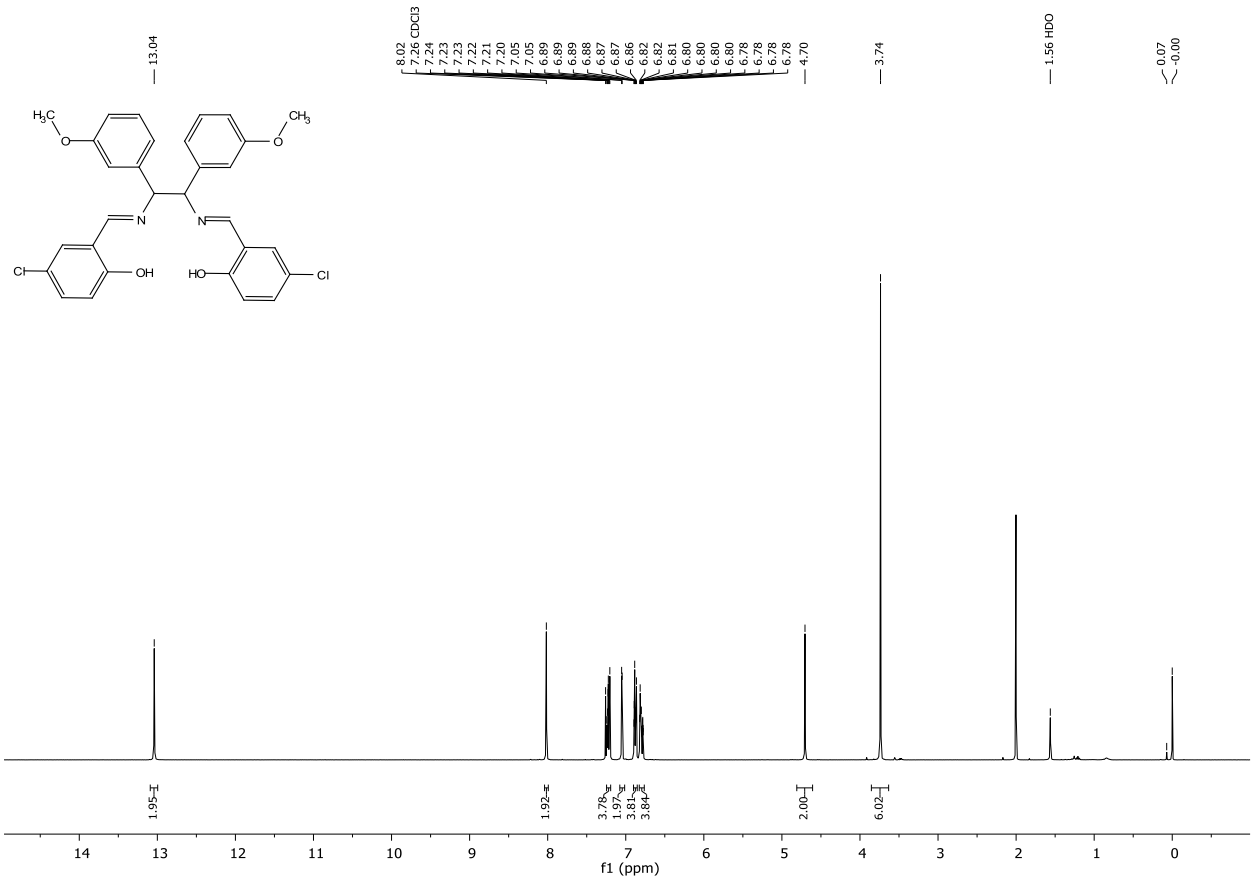


**Figure S2:** $^{1}$H NMR of **L2** in $CDCl_3$

$^{1}$H NMR (400 MHz, $CDCl_3$-*d*) δ 13.04 (s, 2H), 8.02 (s, 2H), 7.27 – 7.18 (m, 4H), 7.05 (d, *J* = 2.5 Hz, 2H), 6.92 – 6.84 (m, 4H), 6.84 – 6.75 (m, 4H), 4.70 (s, 2H), 3.74 (s, 6H)

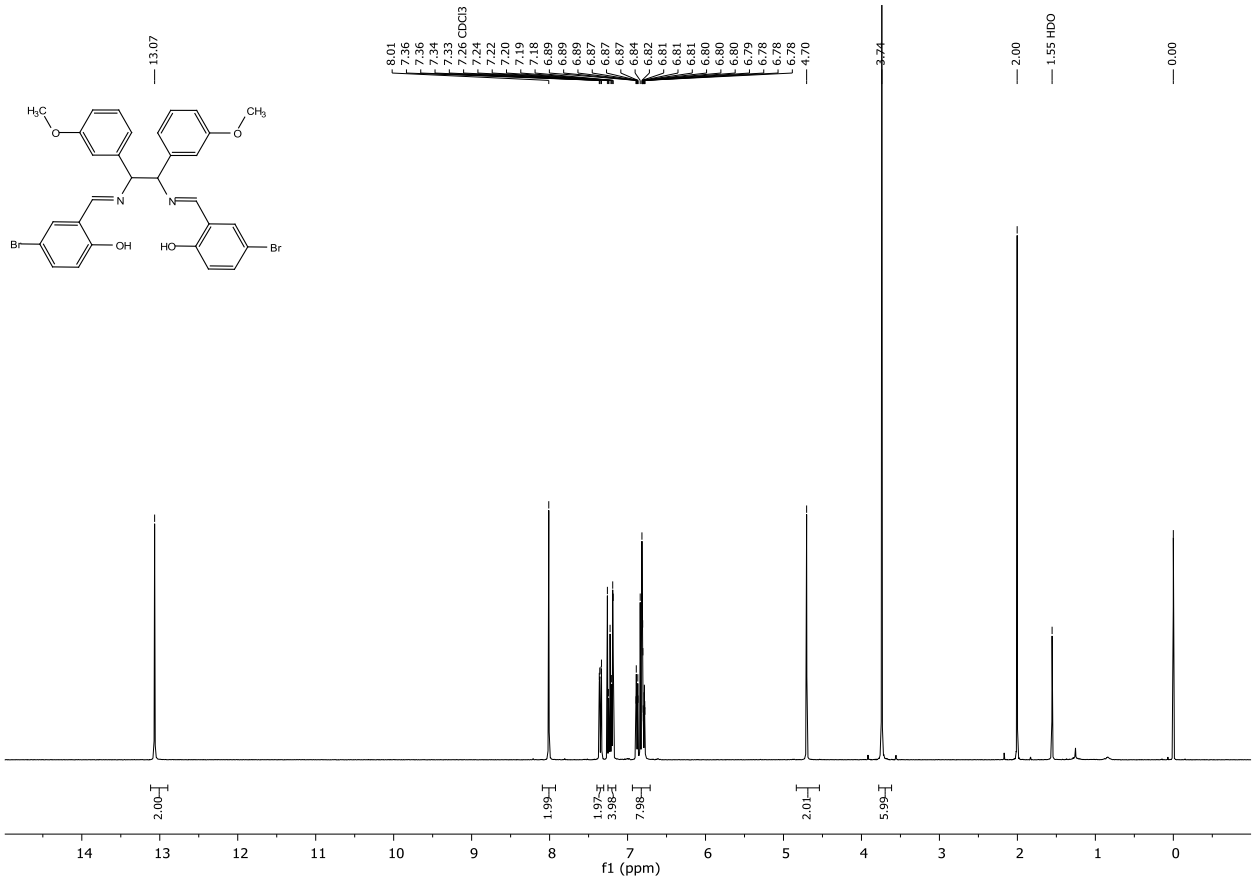


**Figure S3:** $^{1}$H NMR of **L3** in $CDCl_3$

$^{1}$H NMR (400 MHz, $CDCl_3$-*d*) δ 13.07 (s, 2H), 8.01 (s, 2H), 7.35 (dd, *J* = 8.8, 2.5 Hz, 2H), 7.27 – 7.16 (m, 4H), 6.91 – 6.75 (m, 8H), 4.70 (s, 2H), 3.74 (s, 6H)

1.2. $^{13}$C NMR spectra of the ligands

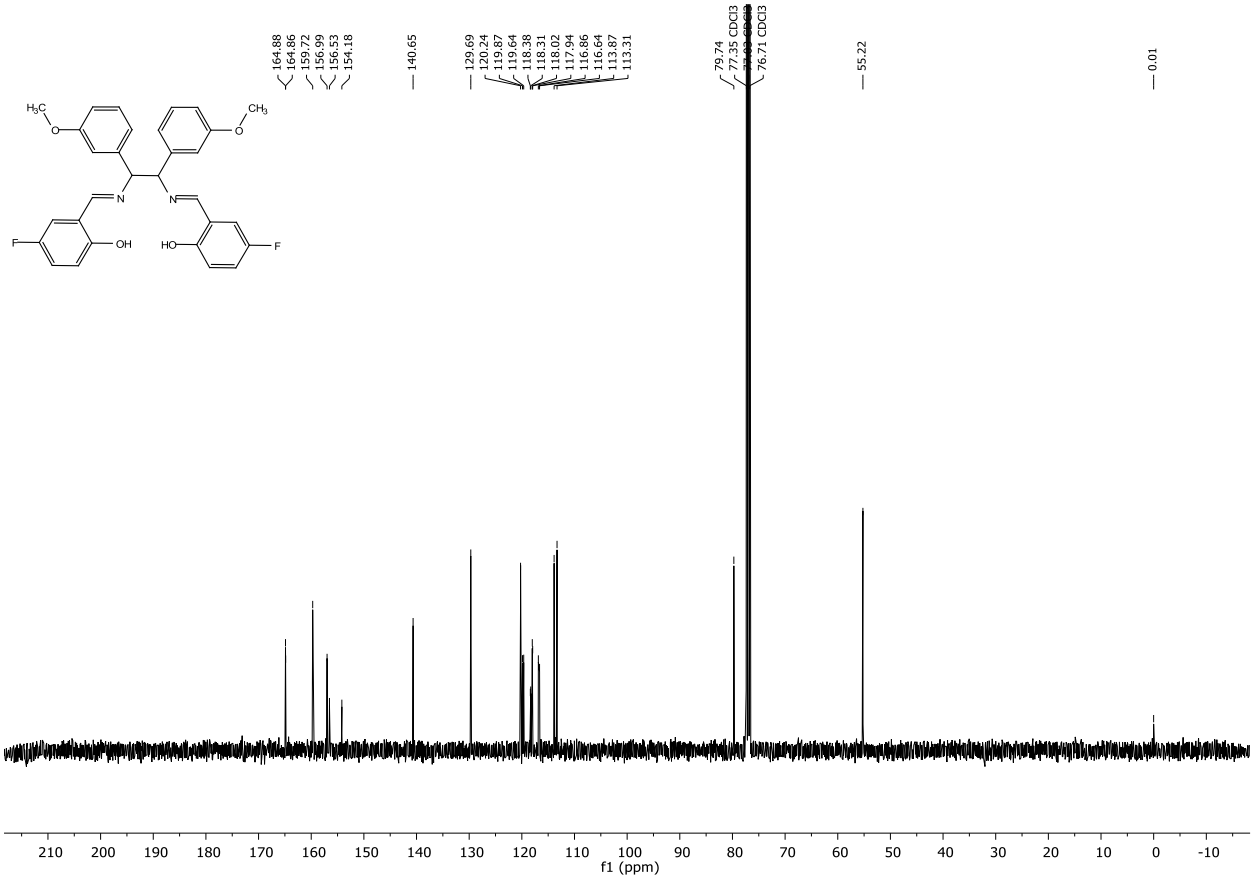


**Figure S4:** $^{13}$C NMR of **L1** in $CDCl_3$

$^{13}$C NMR (101 MHz, $CDCl_3$-*d*) δ 164.87 (d, *J* = 2.7 Hz), 161.75 – 152.15 (m), 140.65, 129.69, 120.24, 119.76 (d, *J* = 23.2 Hz), 118.16 (dd, *J* = 37.0, 7.3 Hz), 116.75 (d, *J* = 22.8 Hz), 113.87, 113.31, 79.74, 55.22

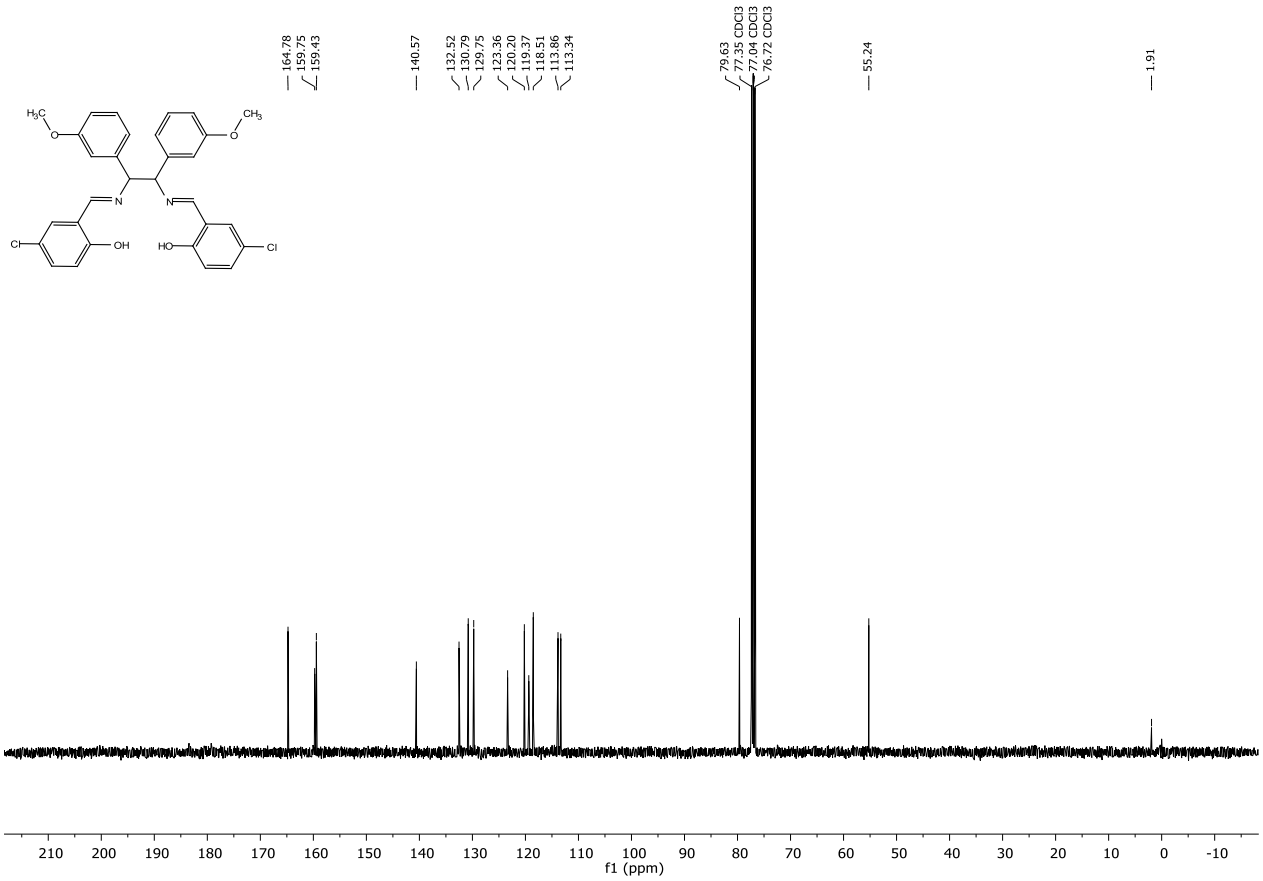


**Figure S5:** $^{13}$C NMR of **L2** in $CDCl_3$

$^{13}$C NMR (101 MHz, $CDCl_3$-*d*) δ 164.78, 159.75, 159.43, 140.57, 132.52, 130.79, 129.75, 123.36, 120.20, 119.37, 118.51, 113.86, 113.34, 79.63, 55.24

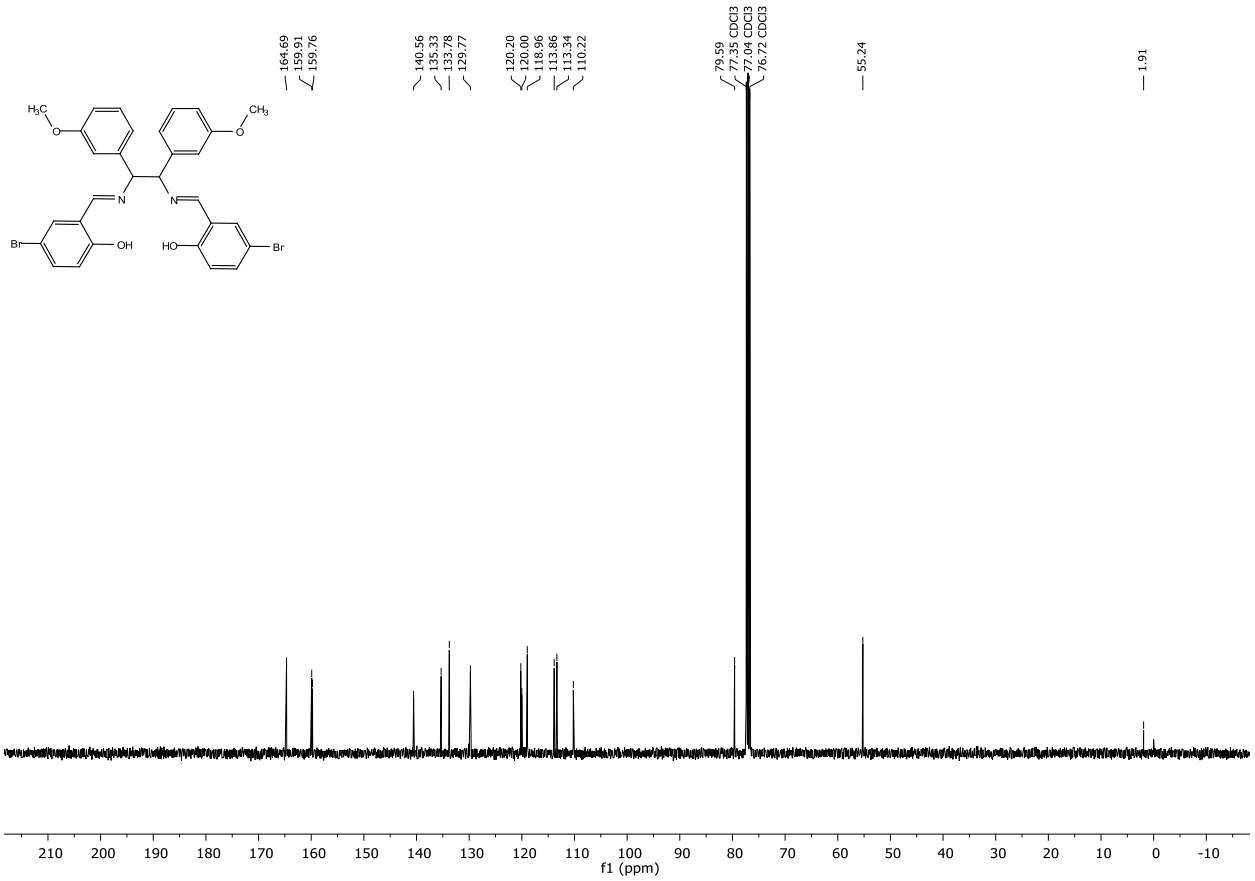


**Figure S6**: $^{13}C$ NMR of **L3** in $CDCl_3$

$^{13}C$ NMR (101 MHz, $CDCl_3$-*d*) δ 164.69, 159.91, 159.76, 140.56, 135.33, 133.78, 129.77, 120.20, 120.00, 118.96, 113.86, 113.34, 110.22, 79.59, 55.24

1.3. $^{1}H$ – $^{13}C$ heteronuclear single quantum correlation (HSQC) of the ligands

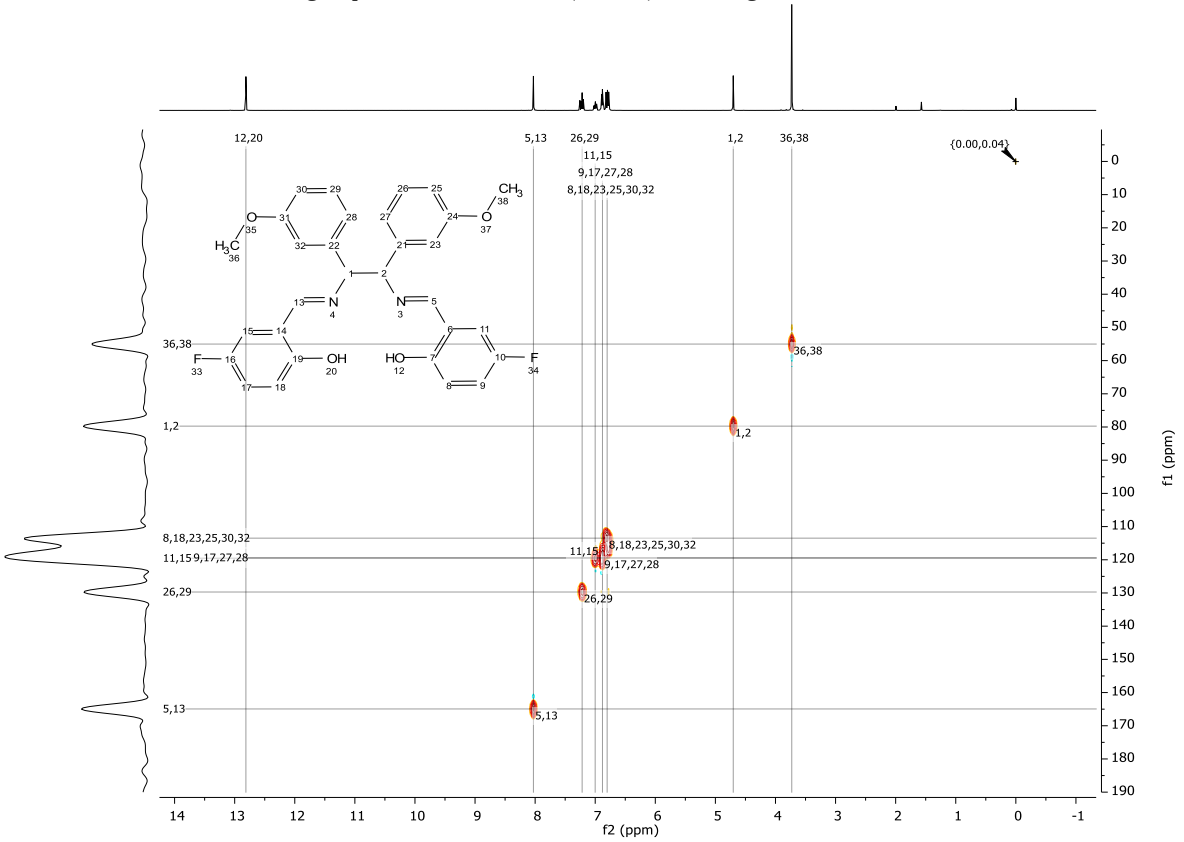


**Figure S7:** $^{1}H$ – $^{13}C$ HSQC spectrum of **L1** in $CDCl_3$

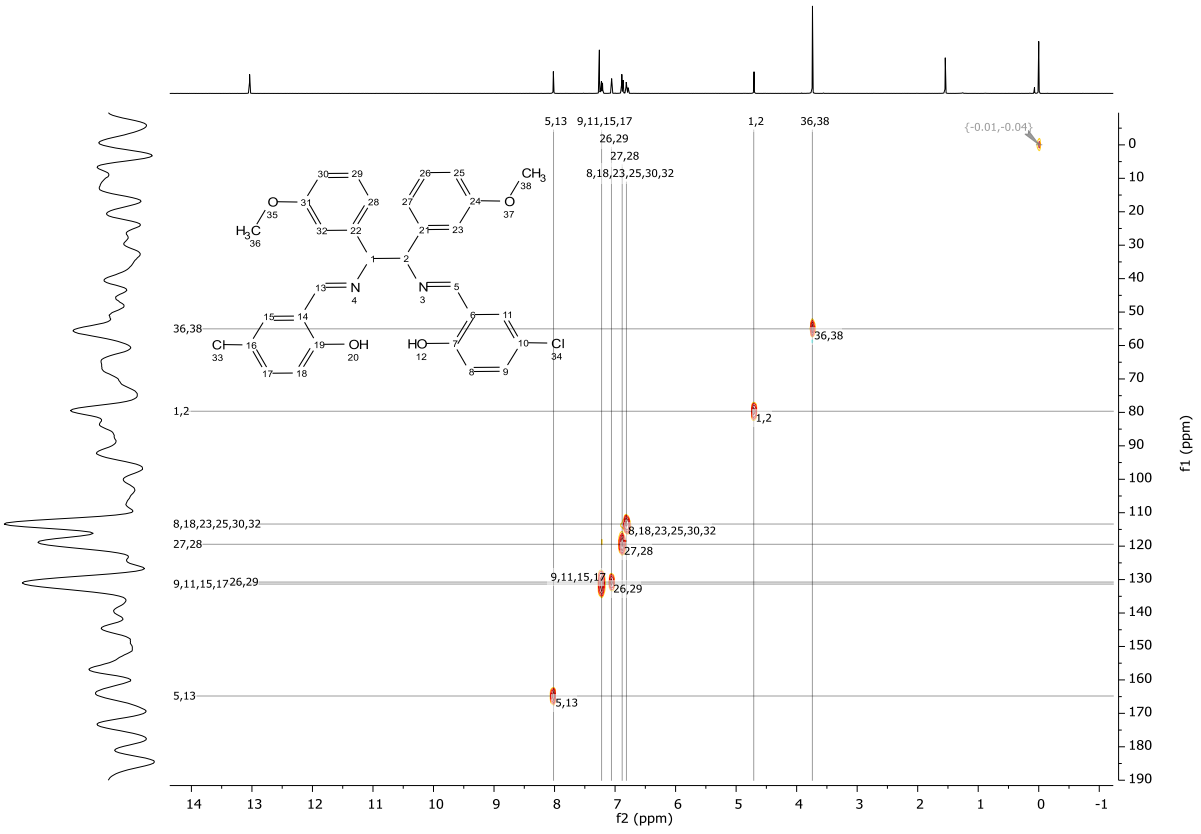


**Figure S8:** $^{1}H$ – $^{13}C$ HSQC spectrum of **L2** in $CDCl_3$

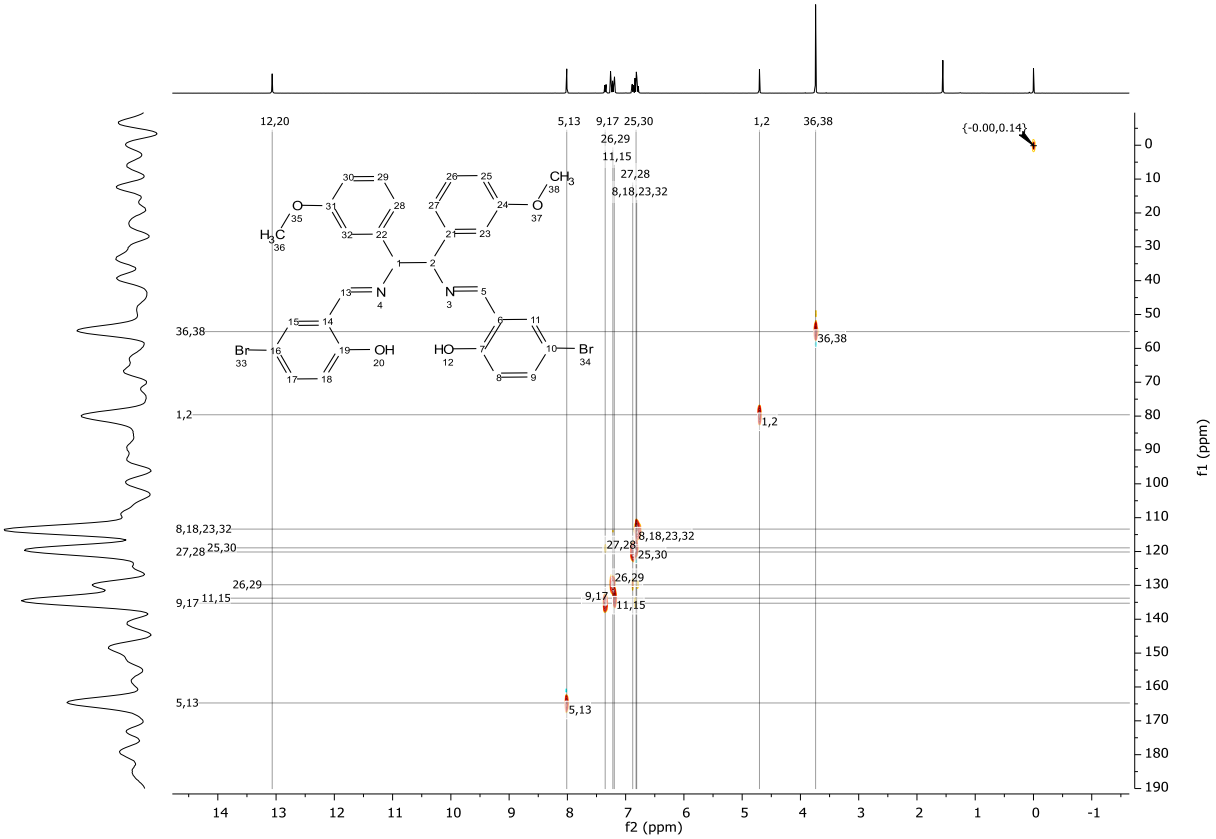


**Figure S9:** $^{1}H$ – $^{13}C$ HSQC spectrum of **L3** in $CDCl_3$

1.4. FT-IR spectra of the ligands

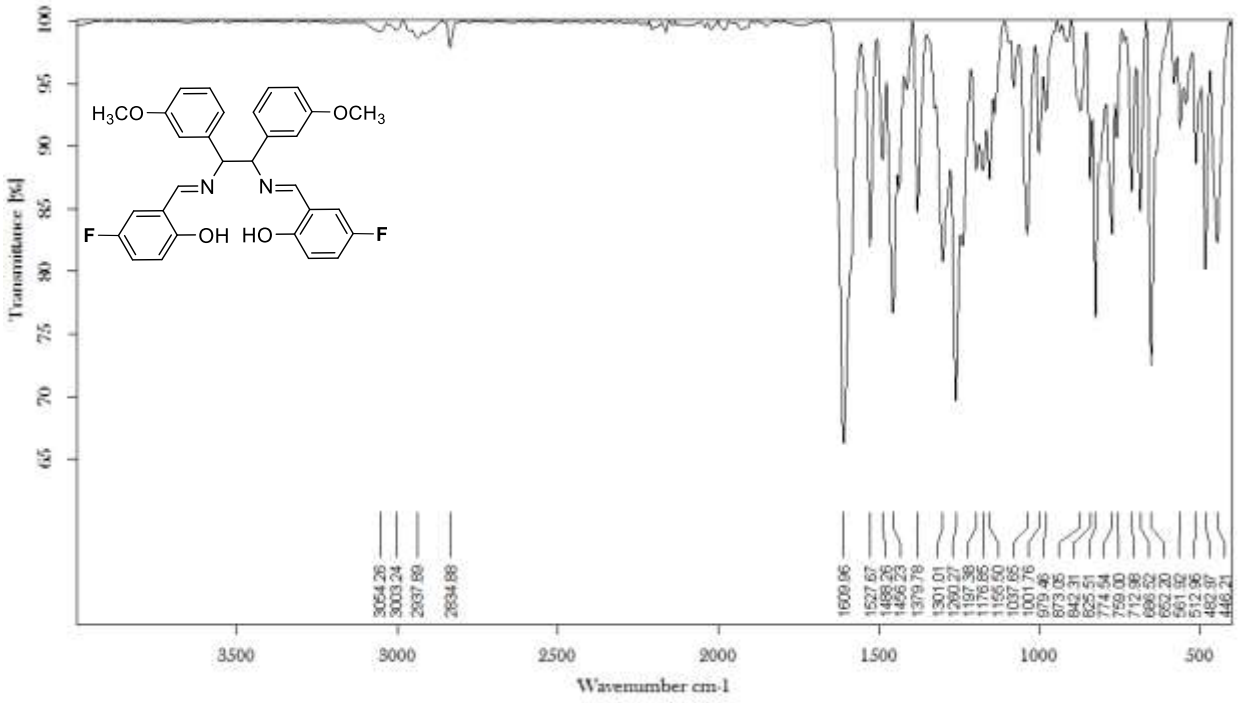


**Figure S10:** FT-IR spectrum of the neat **L1**

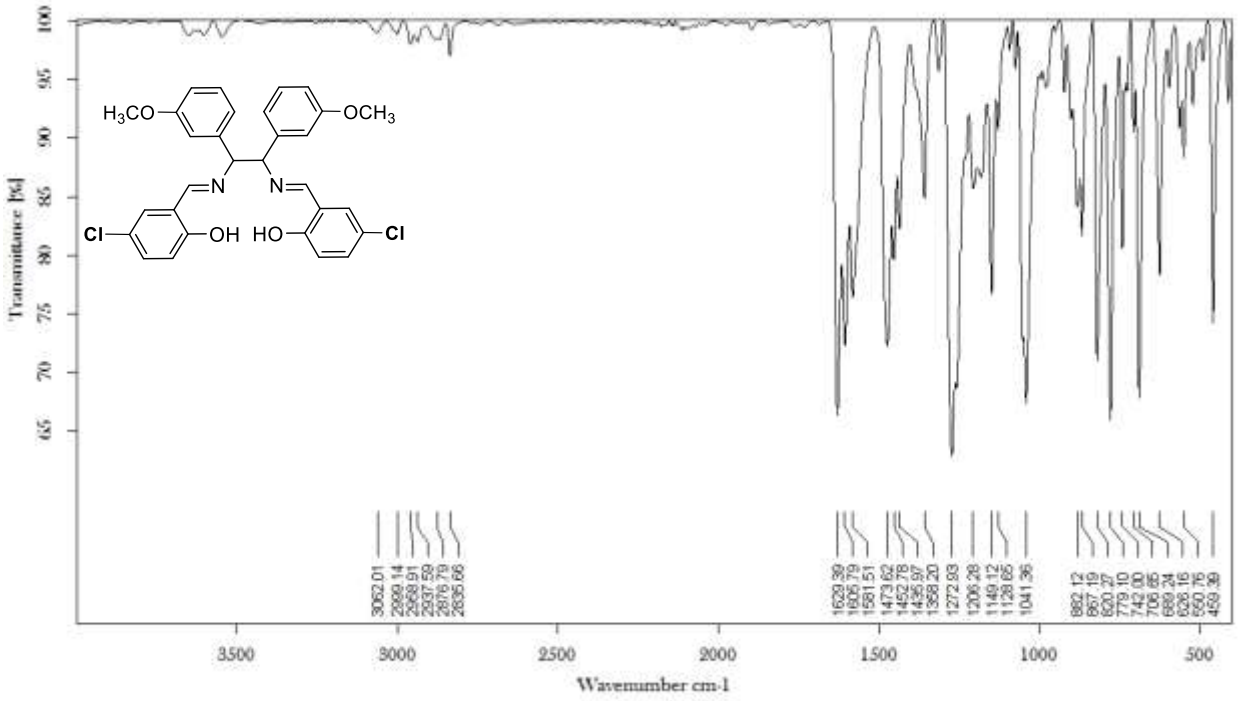


**Figure S11:** FT-IR spectrum of the neat **L2**

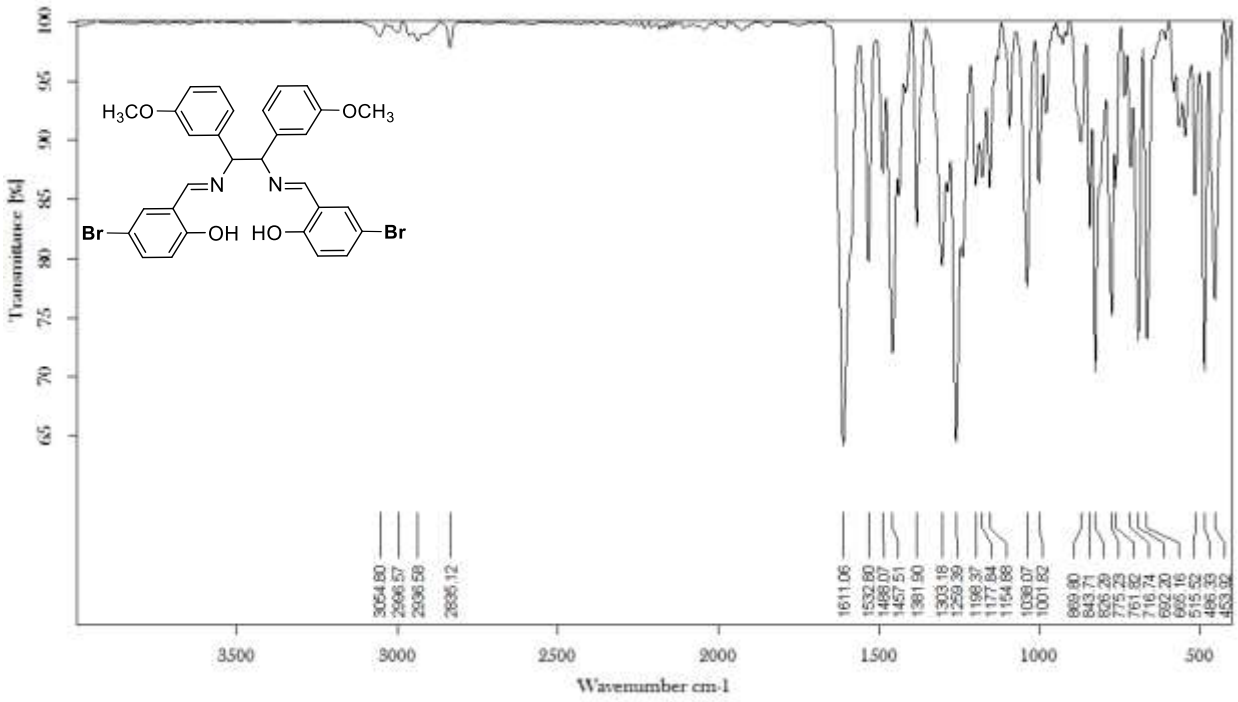


**Figure S12:** FT-IR spectrum of the neat **L3**

1.5. HPLC chromatograms of the ligands

**Table S1:** HPLC data **L1** – **L3**

| Nr. | Ret. Time in Min. | Area % |
|---|---|---|
| **L1** | 2.865 | 96.378 |
| **L2** | 4.713 | 95.724 |
| **L3** | 5.536 | 95.852 |

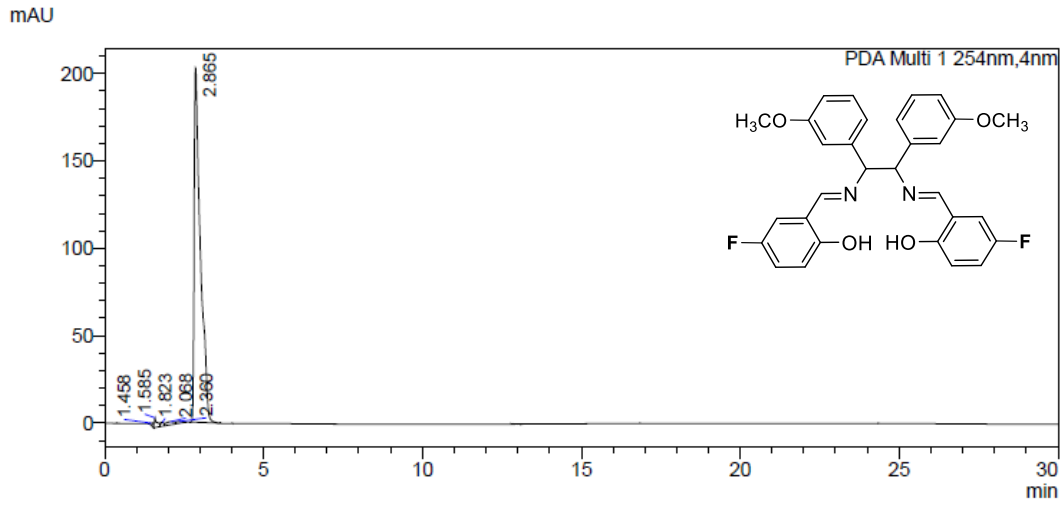


**Figure S13:** HPLC chromatogram of **L1**

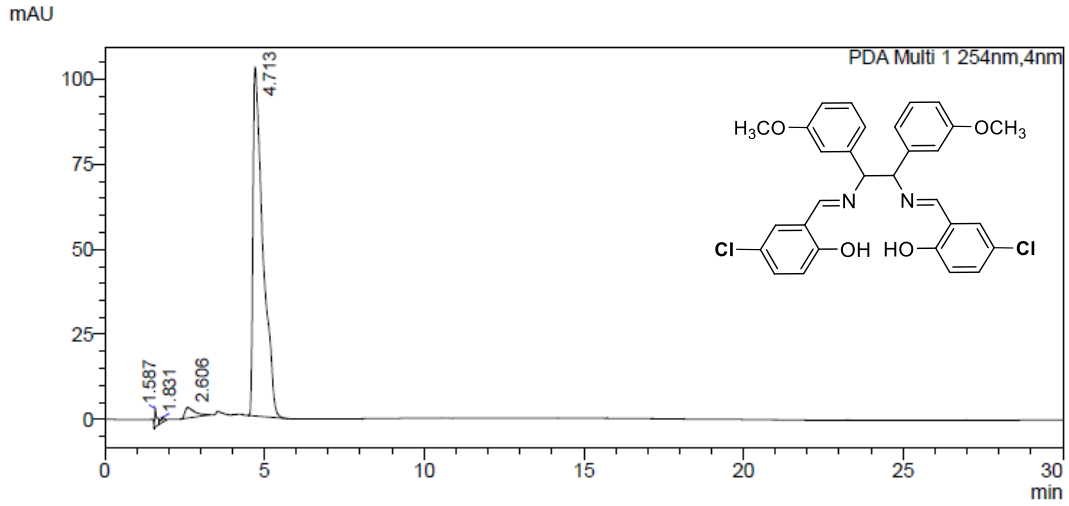


**Figure S14:** HPLC chromatogram of **L2**

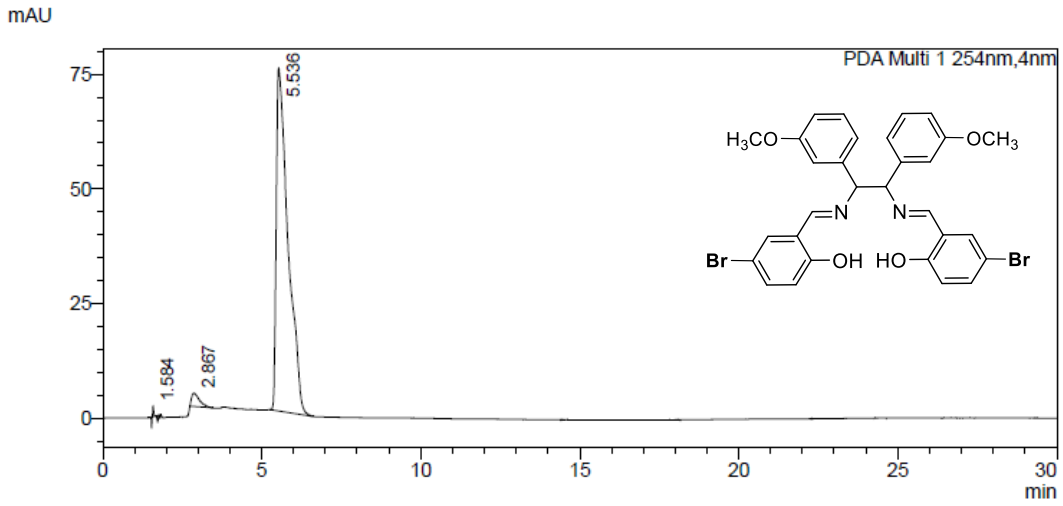


**Figure S15:** HPLC chromatogram of **L3**

## 2. Characterisation of the complexes X1 – X3

2.1. FT-IR spectra of the complexes

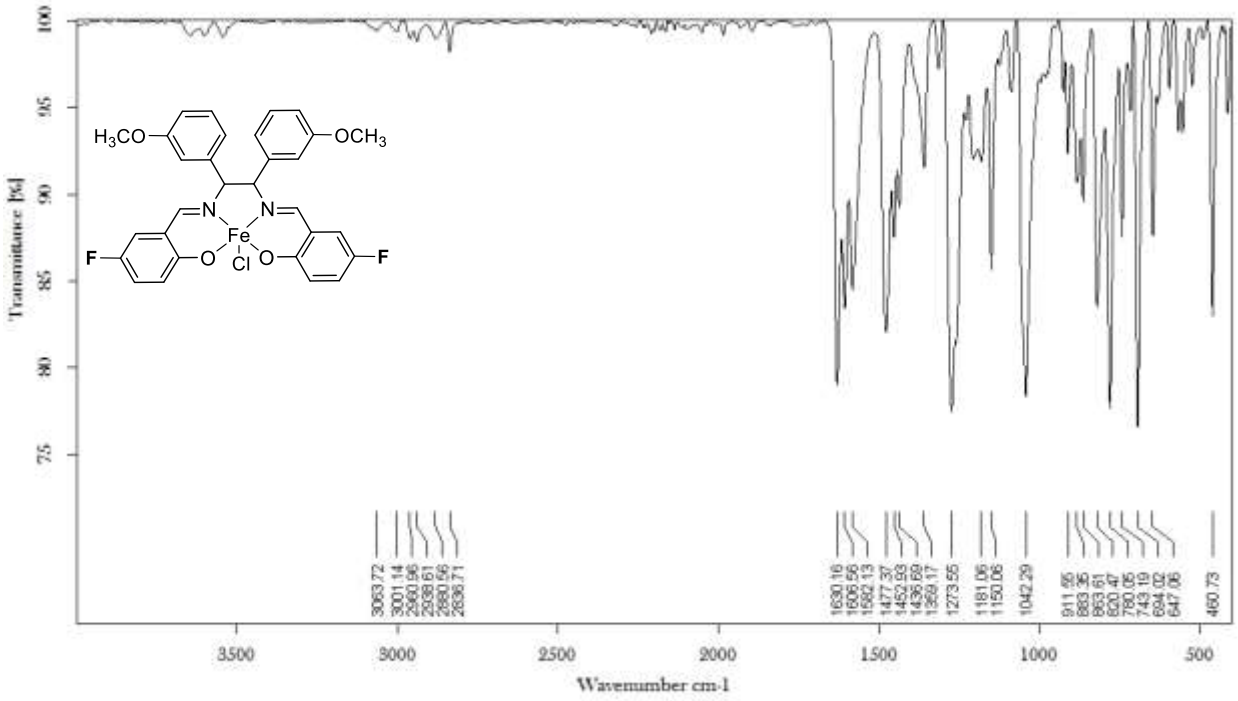


**Figure S16:** FT-IR spectrum of the neat **X1**

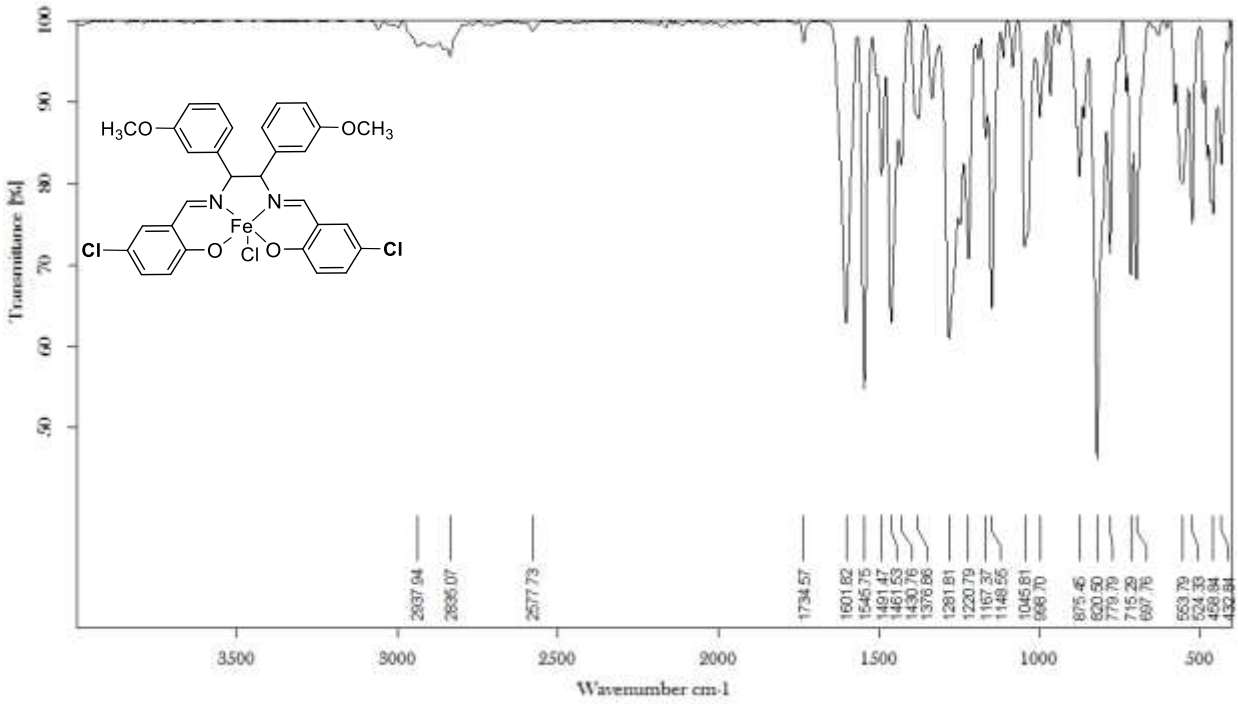


**Figure S17:** FT-IR spectrum of the neat **X2**

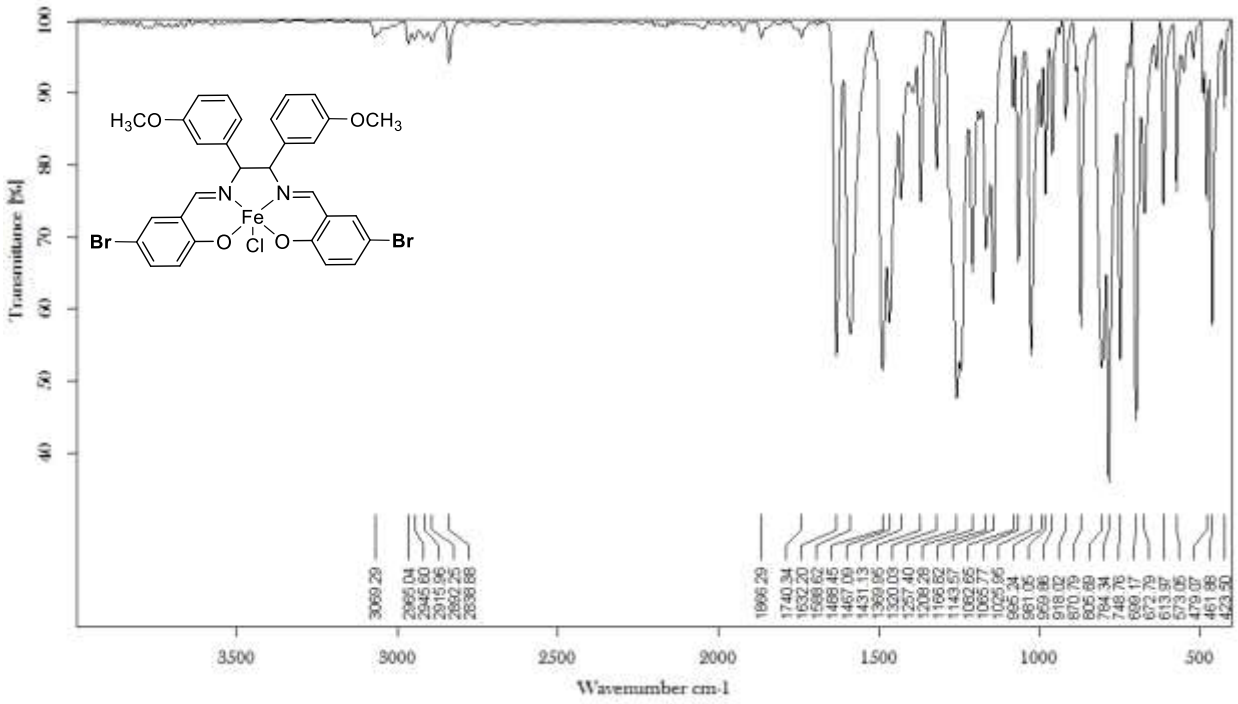


**Figure S18:** FT-IR spectrum of the neat **X3**

2.2. HPLC chromatograms of the complexes

**Table S2:** HPLC data **X1** – **X3**

| Nr. | Ret. Time in Min. | Area % |
|---|---|---|
| **X1** | 4.291 | 99.933 |
| **X2** | 7.614 | 99.794 |
| **X3** | 9.634 | 99.425 |

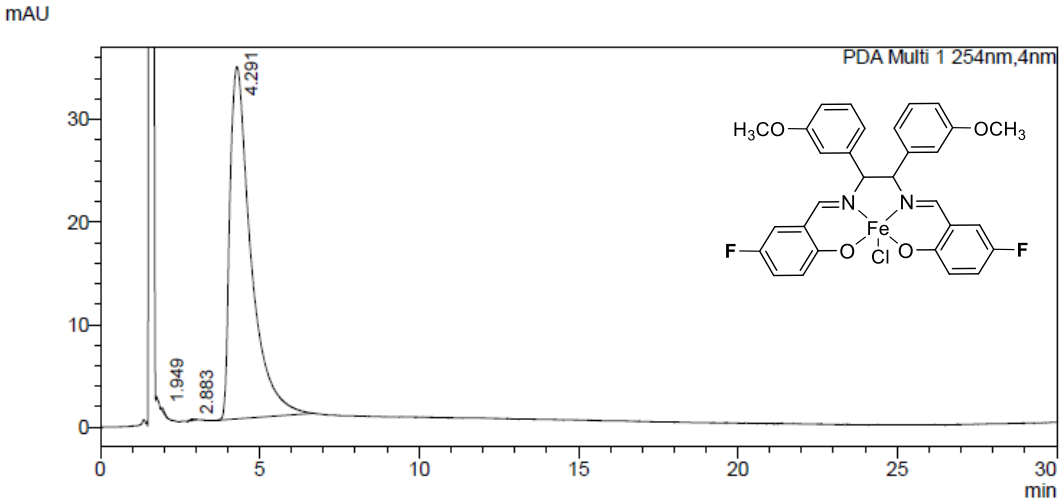


**Figure S19:** HPLC chromatogram of **X1**

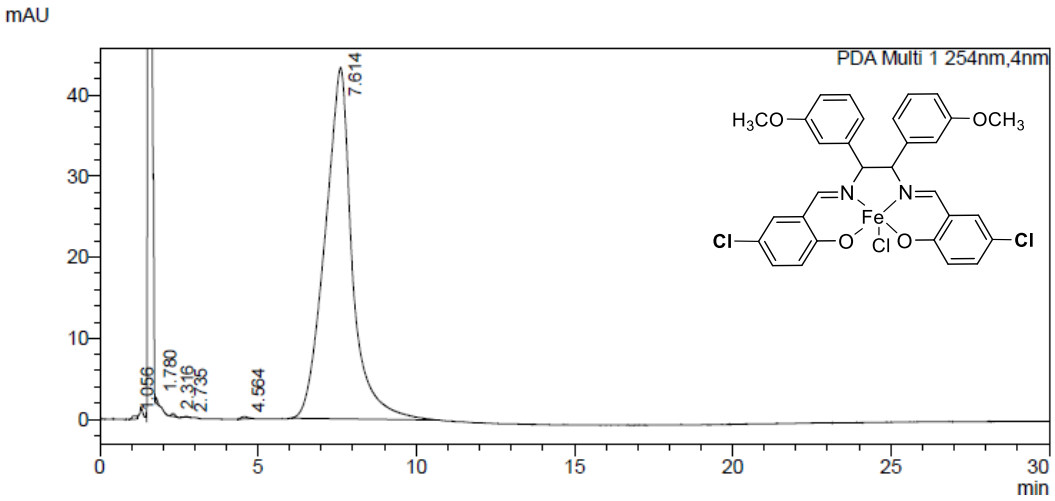


**Figure S20:** HPLC chromatogram of **X2**

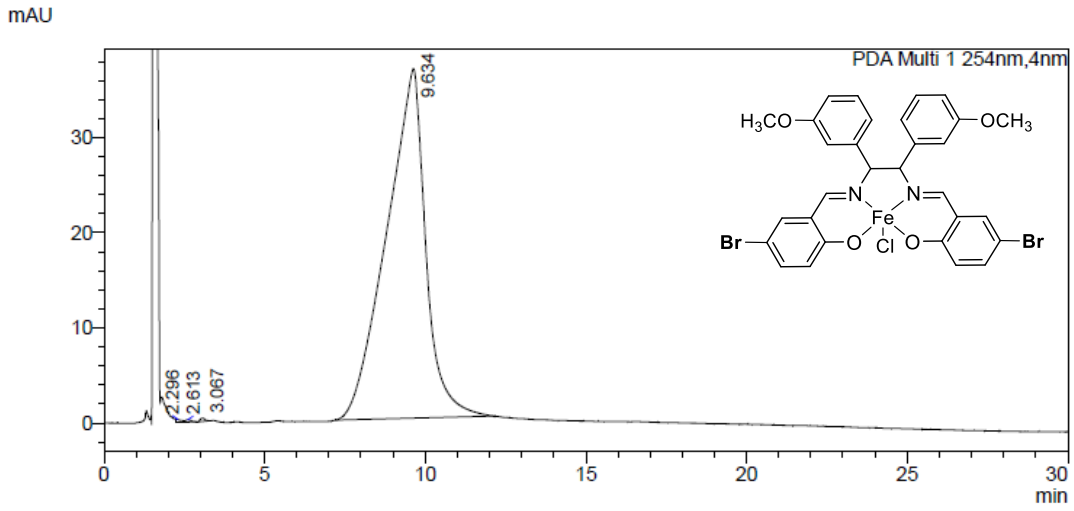


**Figure S21:** HPLC chromatogram of **X3**

2.3. NMR spectra with Evans method of the complexes

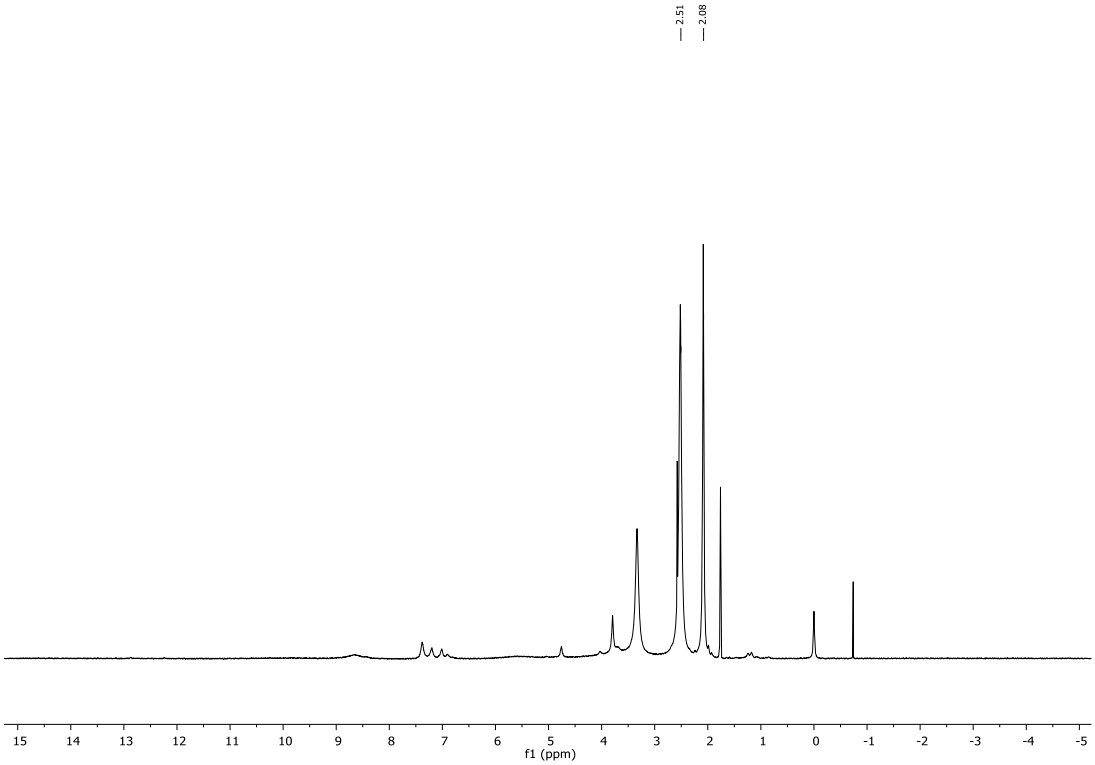


**Figure S22:** [1]H NMR spectrum of 5 mg of paramagnetic **X1** in DMSO-$d_6$ at 298 K with a DMSO-$d_6$ capillary. The shifted and unshifted solvent peaks are highlighted.

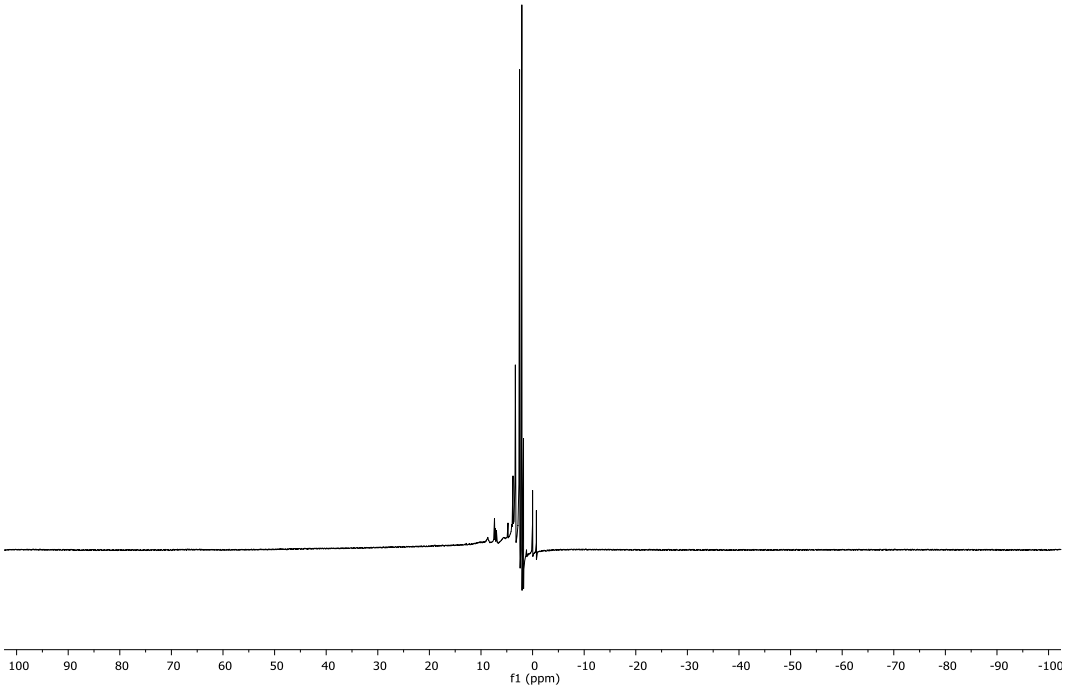


**Figure S23:** [1]H NMR spectrum of 5 mg of paramagnetic **X1** in DMSO-$d_6$ at 298 K

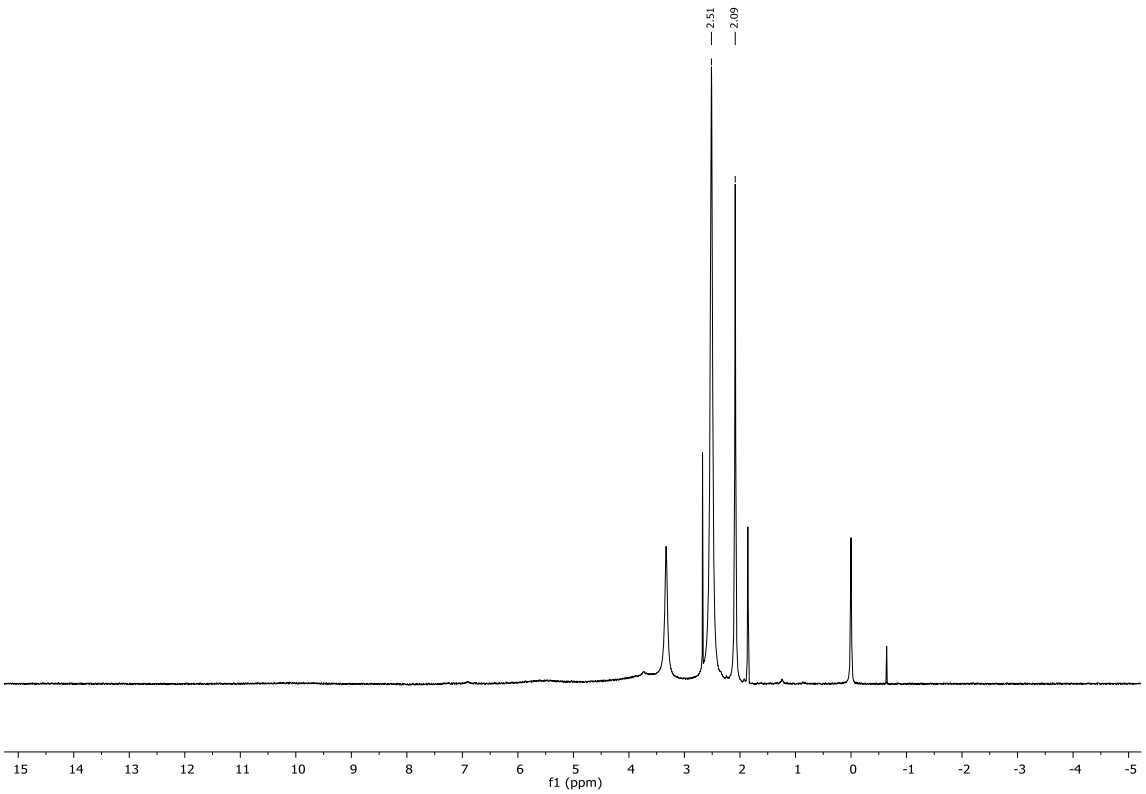


**Figure S24:** $^{1}$H NMR spectrum of 5 mg of paramagnetic **X2** in DMSO-$d_6$ at 298 K with a DMSO-$d_6$ capillary. The shifted and unshifted solvent peaks are highlighted.

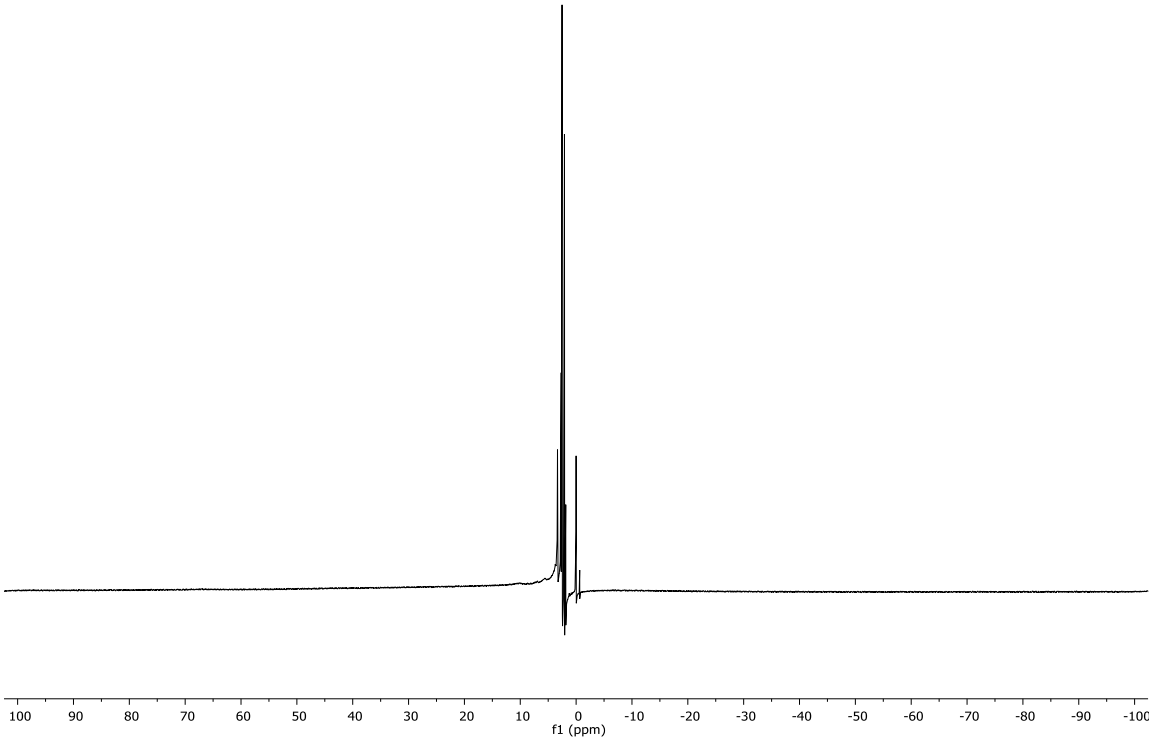


**Figure S25:** $^{1}$H NMR spectrum of 5 mg of paramagnetic **X2** in DMSO-$d_6$ at 298 K

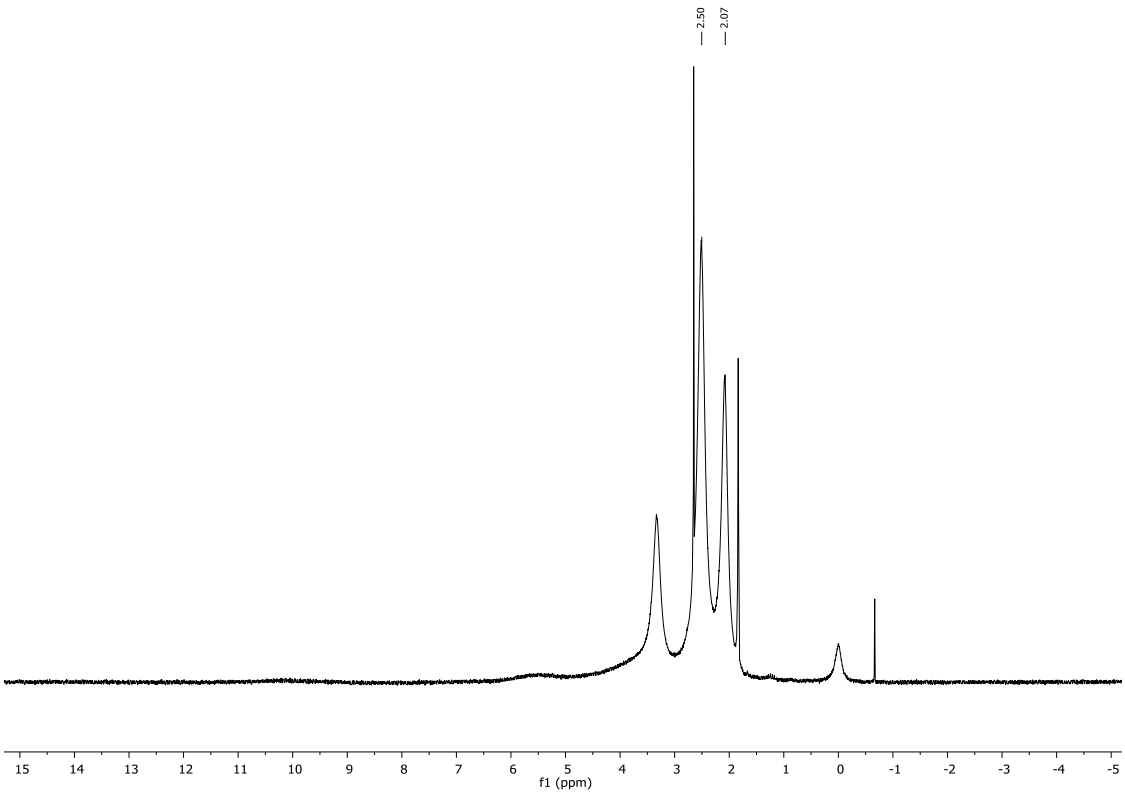


**Figure S26:** $^{1}$H NMR spectrum of 5 mg of paramagnetic **X3** in DMSO-$d_6$ at 298 K with a DMSO-$d_6$ capillary. The shifted and unshifted solvent peaks are highlighted.

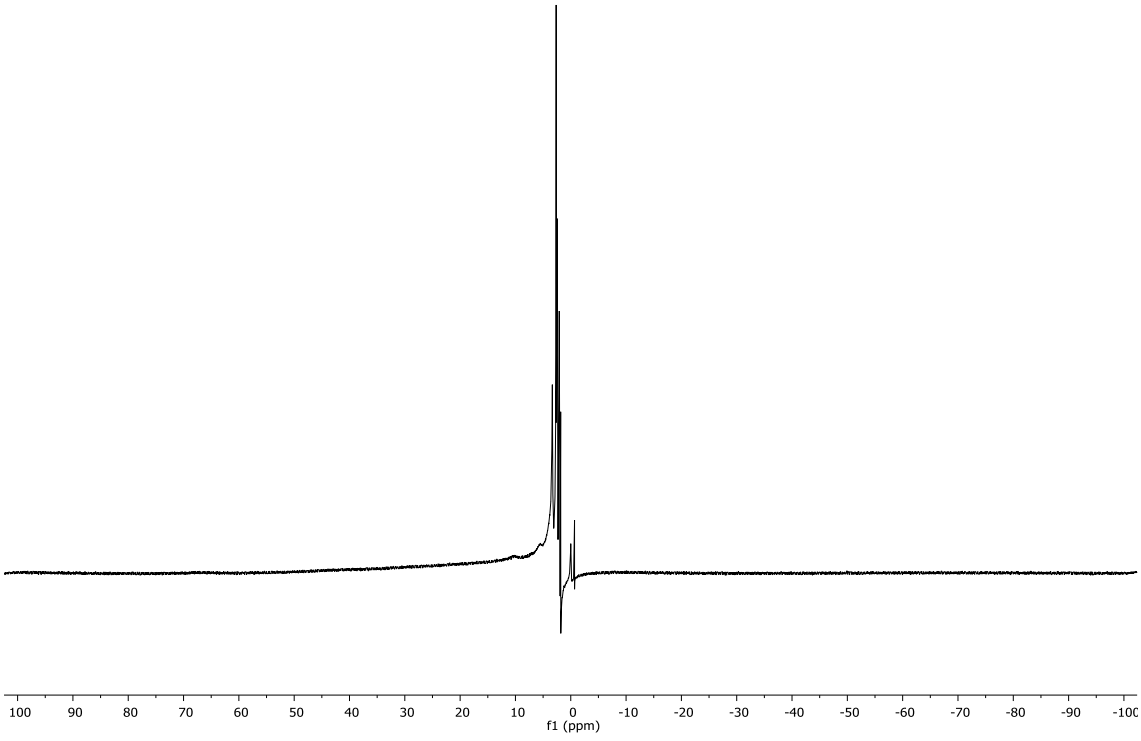


**Figure S27:** $^{1}$H NMR spectrum of 5 mg of paramagnetic **X3** in DMSO-$d_6$ at 298 K

2.4. EPR spectra of the complexes

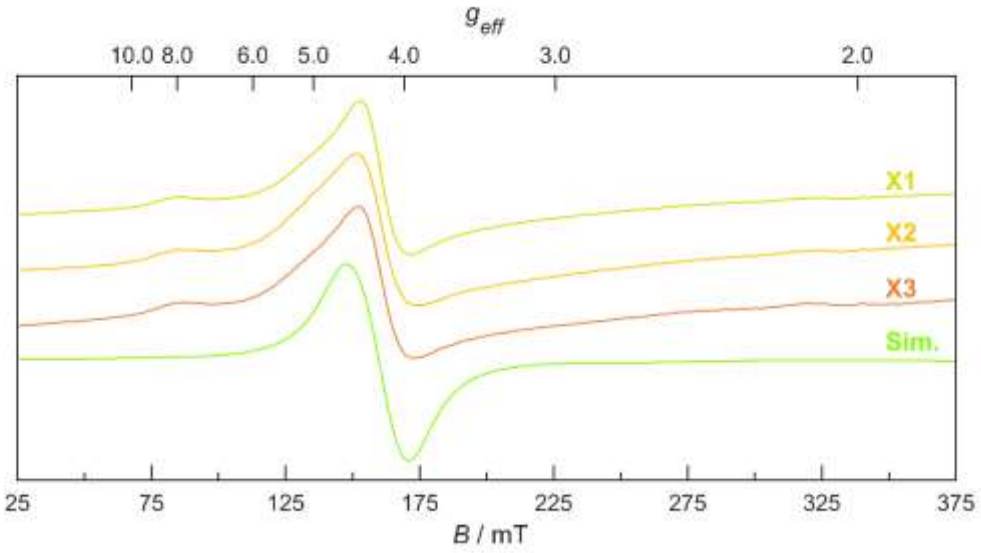


**Figure S28:** EPR spectra of **X1**, **X2** and **X3** in DMSO at 98 K. Simulation of a rhombic spin 5/2 $Fe^{3+}$ system showing the observed signature. Simulation parameters: g_x=g_y=g_z=2.0023, D = 10 000 MHz, E/D = 0.28. Note: The intensity of the signal at g~7.9 is not accurately reproduced in the simulation due to line broadening effects.

## 3. Reactivity toward biological nucleophiles

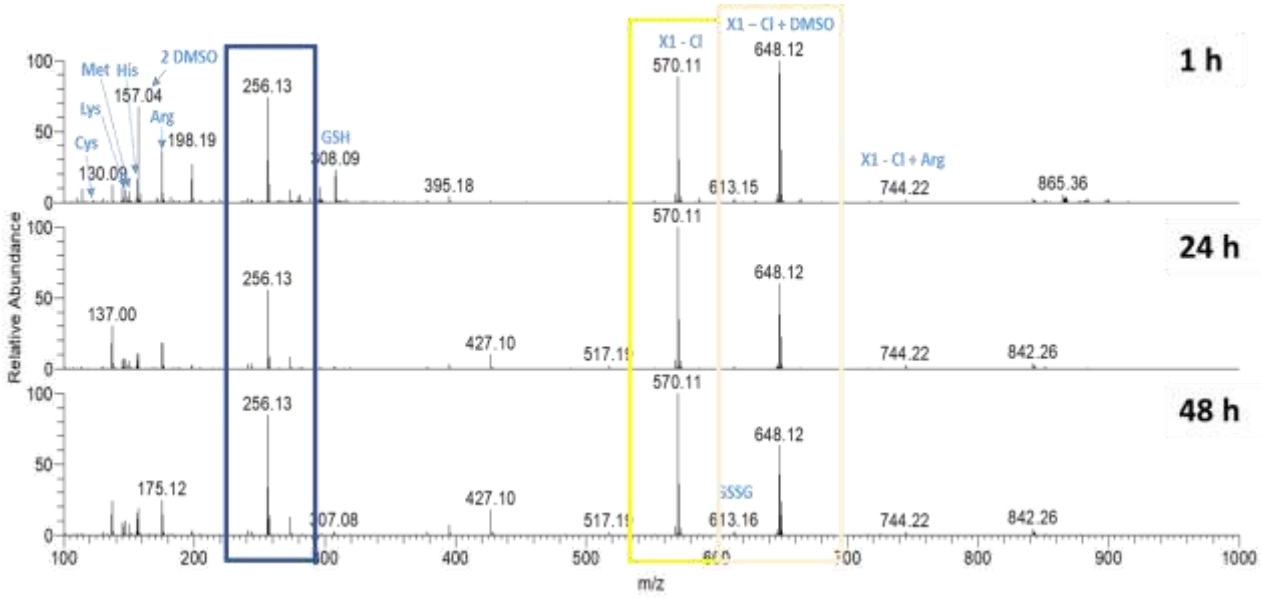


**Figure S29:** HR-MS spectra of **X1** in an aqueous solution containing equimolar amounts of Arg, Cys, His, Lys, Met and GSH.

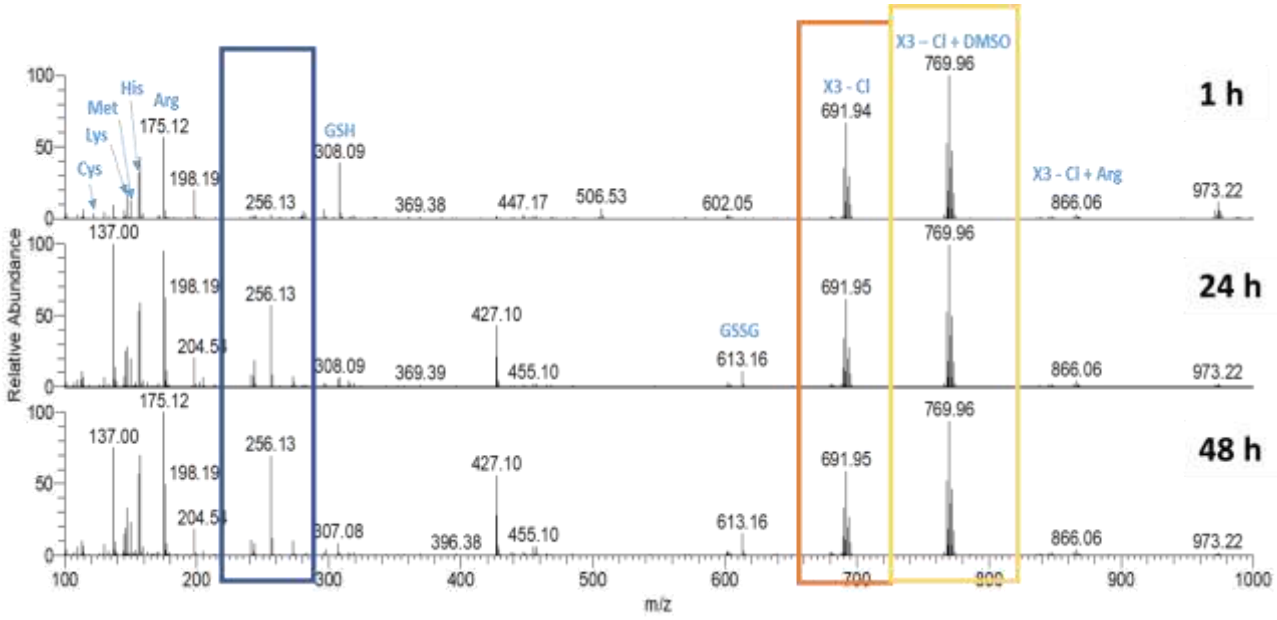


**Figure S30:** HR-MS spectra of **X3** in an aqueous solution containing equimolar amounts of Arg, Cys, His, Lys, Met and GSH.

**Table S3:** List of ions observed in the HR-MS analysis of **X1** – **X3** in aqueous solution. Oleamide is a common contaminant.

| | species | $m_{exp.}$ | $m_{calc}$ | error [ppm] |
|---|---|---|---|---|
| **biomolecules** | $[Cys + H]^+$ | 122.0272 | 122.0270 | 1.64 |
| | $[Lys + H]^+$ | 147.1130 | 147.1128 | 1.36 |
| | $[Met + H]^+$ | 150.0585 | 150.0583 | 1.33 |
| | $[His + H]^+$ | 156.0769 | 156.0768 | 0.64 |
| | $[Arg + H]^+$ | 175.1191 | 175.1190 | 0.57 |
| | $[GSH + H]^+$ | 308.0914 | 308.0911 | 0.97 |
| | $[GSSG + H]^+$ | 613.1604 | 613.1592 | 1.96 |
| **hydrolysis products** | $[C_{16}H_{17}O_2N + H]^+$ | 256.1336 | 256.1332 | 1.56 |
| | $[C_{16}H_{20}O_2N_2 + H]^+$ | 273.1602 | 273.1598 | 1.46 |
| | $[C_{23}H_{20}O_3N_1Cl + H]^+$ | 394.1212 | 394.1204 | 2.03 |
| | $[C_{23}H_{23}O_3N_2Cl + H]^+$ | 411.1478 | 411.1470 | 1.95 |
| **X1** | $[X1 - Fe - Cl + 3H]^+$ | 517.1943 | 517.1933 | 1.93 |
| | $[X1 - Cl]^+$ | 570.1057 | 570.1049 | 1.40 |
| | $[X1 - Cl + DMSO]^+$ | 648.1198 | 648.1190 | 1.23 |
| | $[X1 - Cl + Lys]^+$ | 716.2118 | 716.2104 | 1.95 |
| | $[X1 - Cl + His]^+$ | 725.1758 | 725.1741 | 2.34 |
| | $[X1 - Cl + Arg]^+$ | 744.2180 | 744.2167 | 1.75 |
| | $[X1 - Cl + C_{16}H_{20}O_2N_2]^+$ | 842.2592 | 842.2573 | 2.26 |
| | $[X1 - Cl + GSH]^+$ | 877.1903 | 877.1888 | 1.71 |
| **X2** | $[X2 - Cl]^+$ | 602.0470 | 602.0457 | 2.16 |
| | $[X2 - Cl + DMSO]^+$ | 680.0611 | 680.0596 | 2.21 |
| | $[X2 - Cl + Lys]^+$ | 748.1531 | 748.1512 | 2.54 |
| | $[X2 - Cl + His]^+$ | 757.1170 | 757.1152 | 2.38 |
| | $[X2 - Cl + Arg]^+$ | 776.1594 | 776.1574 | 2.58 |
| | $[X2 - Cl + oleamide]^+$ | 883.3197 | 883.3174 | 2.60 |
| | $[X2 - Cl + GSH]^+$ | 909.1316 | 909.1295 | 2.31 |
| **X3** | $X3 - Cl]^+$ | 691.9440 | 691.9426 | 2.02 |
| | $[X3 - Cl + DMSO]^+$ | 769.9585 | 769.9566 | 2.47 |
| | $[X3 - Cl + Lys]^+$ | 838.0500 | 838.0482 | 2.15 |
| | $[X3 - Cl + His]^+$ | 847.0140 | 847.0121 | 2.24 |
| | $[X3 - Cl + Arg]^+$ | 866.0563 | 866.0543 | 2.31 |
| | $[X3 - Cl + oleamide]^+$ | 973.2168 | 973.2145 | 2.36 |
| | $[X3 - Cl + GSH]^+$ | 999.0286 | 999.0264 | 2.20 |

## 4. Biological activity

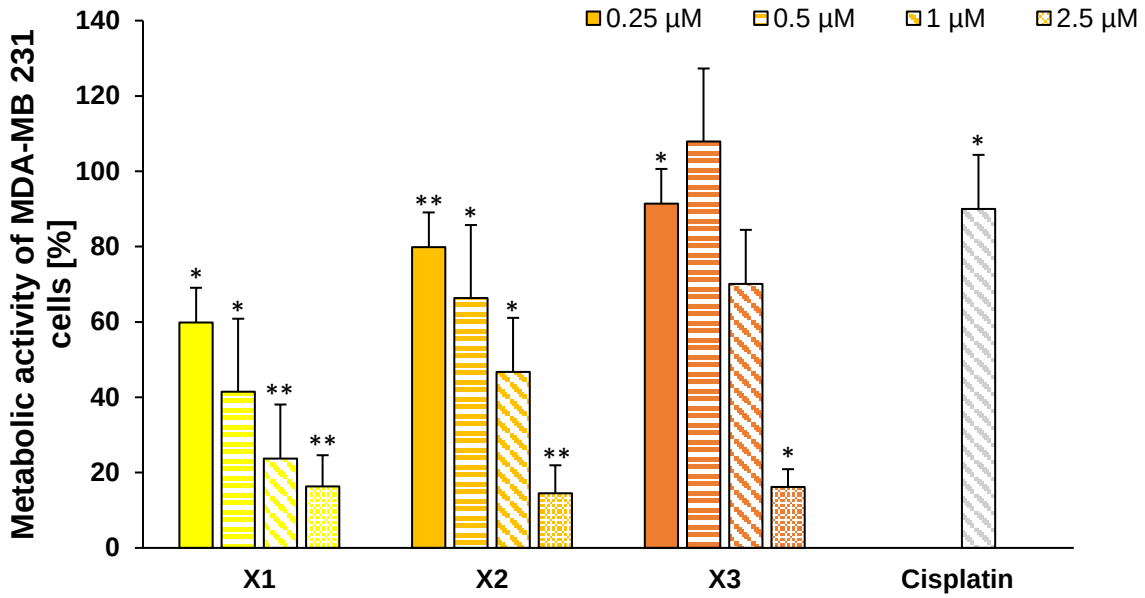


**Figure S31:** Effect of the iron(III) salene complexes **X1** – **X3** on the metabolic activity of MDA-MB 231. The mean proliferation + SE of eight independent experiments is plotted. The metabolic activity of cells only (without compound) was set at 100% (data not shown). The asterisks (* $p<0.05$, ** $p<0.005$ against no compound) represents statistical significance.

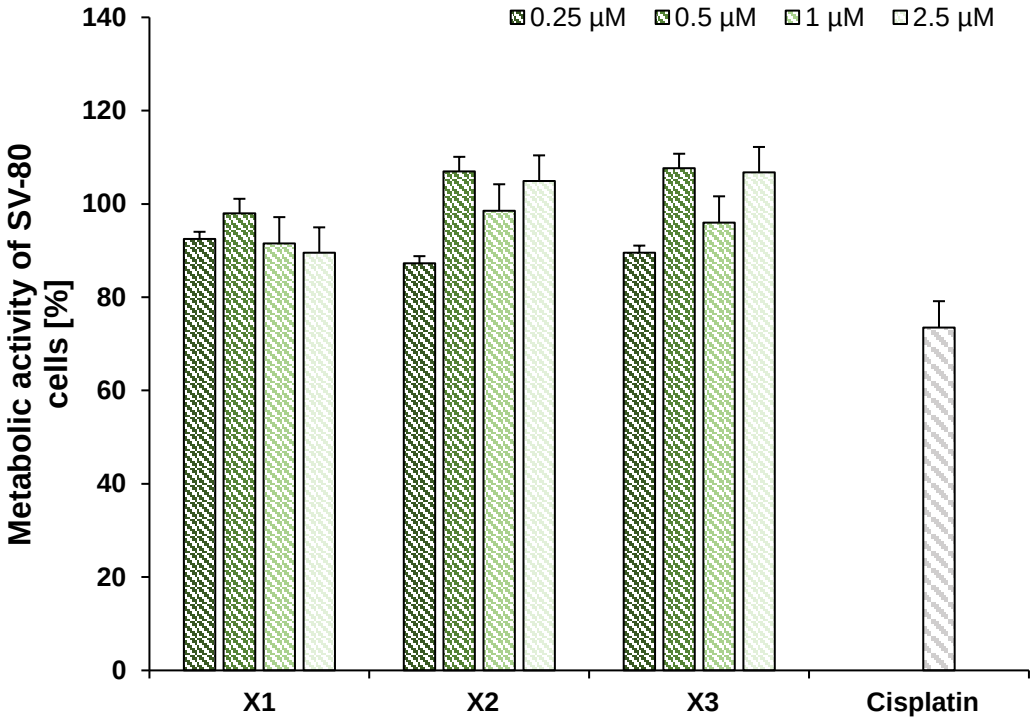


**Figure S32:** Effect of the iron(III) salene complexes **X1** – **X3** on the metabolic activity of SV-80 transformed fibroblasts. The mean metabolic activity + SE of five independent experiments is plotted. The metabolic activity of cells only (without compound) was set at 100%.

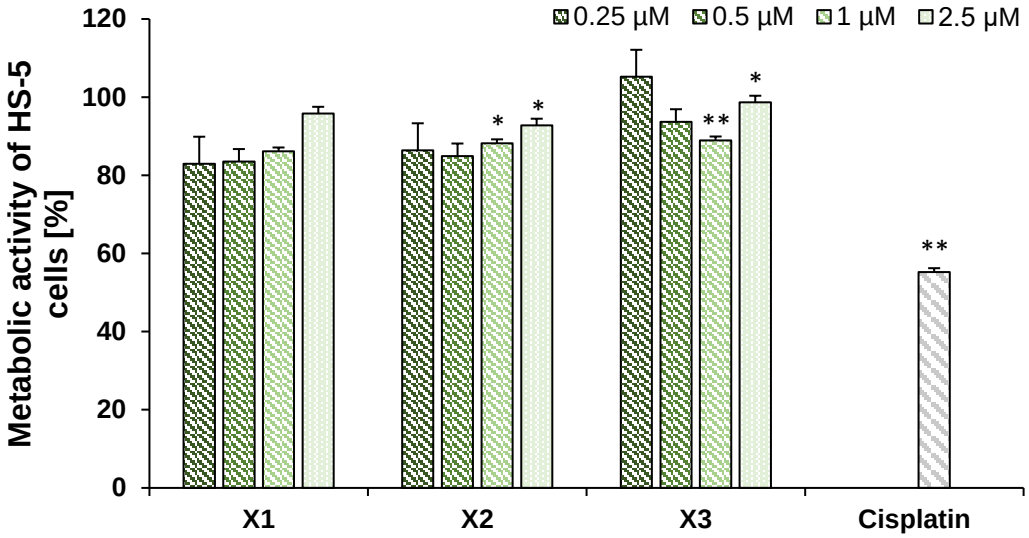


**Figure S33:** Effect of the iron(III) salene complexes **X1** – **X3** on the metabolic activity of HS-5 cells. The mean metabolic activity + SE of six independent experiments is plotted. The metabolic activity of cells only (without compound) was set at 100%. The asterisks (* $p<0.05$, ** $p<0.005$ against no compound) represents statistical significance.

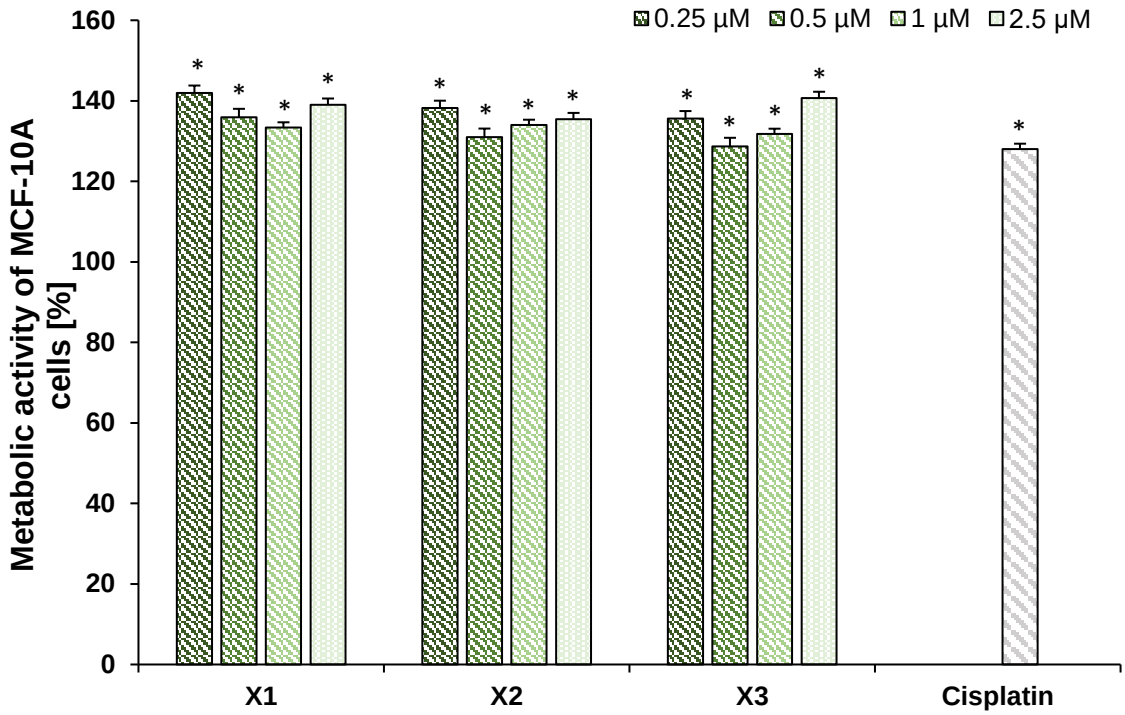


**Figure S34:** Effect of the iron(III) salene complexes **X1** – **X3** on the metabolic activity of MCF-10A cells. The mean metabolic activity + SE of six independent experiments is plotted. The metabolic activity of cells only (without compound) was set at 100%. The asterisks (* $p<0.005$ against no compound) represent statistical significance.